nature communications

Article

https://doi.org/10.1038/s41467-025-59908-7

Evolutionary origins of self-sustained Kai protein circadian oscillators in cyanobacteria

Received: 16 August 2024

Accepted: 2 May 2025

Published online: 15 May 2025

Check for updates

Atsushi Mukaiyama[1,6] ✉, Yoshihiko Furuike[2,3,6] ✉, Kumiko Ito-Miwa[4], Yasuhiro Onoue[2], Kota Horiuchi[2,3], Kanta Kondo[2,3], Eiki Yamashita[5] & Shuji Akiyama[2,3] ✉

Light–dark cycles affect photosynthetic efficiency in autotrophic cyanobacteria; therefore, determining whether ancient cyanobacteria possessed a self-sustained circadian clock when oxygenic photosynthetic systems were established is an important issue in chronobiology. Here we examine the oscillation of the clock protein KaiC in modern cyanobacteria, as well as the function and structure of ancestral Kai proteins, to determine the evolutionary origin of the self-sustained Kai-protein oscillators. The results show that the oldest double-domain KaiC in ancestral bacteria lacks the factors functionally and structurally essential for rhythmicity. The ancestral Kai proteins have acquired these factors through molecular evolution that occurred around Global Oxidation and Snowball Earth events, and are eventually inherited as a self-sustained circadian oscillator by the most recent common ancestor of cyanobacteria capable of oxygenic photosynthesis. This autonomous Kai protein oscillator is further inherited by most freshwater and marine cyanobacteria present today as an autotrophic basis for time-optimal acquisition and consumption of energy from oxygenic photosynthesis.

The most recent common ancestor (MRCA) of cyanobacteria emerged approximately 3–2 billion years (Ga) ago[1–6] and evolved into the current ecosystem through the Great Oxidation event (GOE) 2.3 Ga ago[7], at least two Snowball Earth events (SEEs) 2.4 and 0.7 Ga ago[8–10], and the Neoproterozoic Oxygenation event (NOE) 0.8–0.6 Ga ago[11,12]. Studies of fossils and molecular evolution models suggest that the MRCA of cyanobacteria already possessed primitive oxygenic photosynthetic systems[1,2,4]. Because the efficiency of photosynthesis is strongly influenced by light–dark environmental cycles, determining whether primitive cyanobacteria possessed a time-keeping system when photosynthesis became active in the GOE period is important to understanding the physiological origin of circadian clock systems[13]. Primitive biological clocks are also of interest from the perspective of geoscience, and the evolution of the Earth's rotation period from ancient times to the present remains an issue of debate[14].

Circadian clocks with autonomous 24-h oscillatory, temperature compensatory, and synchronous properties have been identified in various extant organisms[15], including bacteria[16], fungi[17], plants[18], and mammals[19]. The circadian clock of cyanobacteria has been studied intensively using the *Synechococcus elongatus* PCC7942 (*Se*7942) strain as a model system[20,21]. The clock oscillator can be reconstructed in a test tube by incubating the core protein KaiC from the *Se*7942 strain (KaiC^{Se}) in the presence of KaiA^{Se}, KaiB^{Se}, and adenosine triphosphate (ATP)[22]. KaiC^{Se} exhibits rhythms in phosphorylation[23,24] and interactions with KaiA^{Se} and KaiB^{Se}[25–28]; however, the frequency of these rhythms is highly correlated with the ATPase activity of KaiC^{Se} itself[29,30]. For example, when the ATPase activity of KaiC^{Se} doubles as a result of

[1]Department of Bioscience and Biotechnology, Fukui Prefectural University, Eiheiji 910-1195, Japan. [2]Research Center of Integrative Molecular Systems (CIMoS), Institute for Molecular Science, National Institutes of Natural Sciences, Okazaki 444–8585, Japan. [3]Molecular Science Program, Graduate University for Advanced Studies, SOKENDAI, Okazaki 444-8585, Japan. [4]Graduate School of Science and Institute for Advanced Research, Nagoya University, Nagoya 464-8602, Japan. [5]Institute for Protein Research, The University of Osaka, Suita 565-0871, Japan. [6]These authors contributed equally: Atsushi Mukaiyama, Yoshihiko Furuike. ✉e-mail: amukai@fpu.ac.jp; furuike@ims.ac.jp; akiyamas@ims.ac.jp

amino acid substitutions, the frequencies of both the in vitro oscillator and the intracellular rhythm also double. This process mediated by KaiC^{Se} is known as cross-scale causality and is also observed in temperature compensation[31].

One hypothesis worth testing is whether primitive cyanobacteria utilized a Kai-protein oscillator. However, the concept of a protein-based oscillator is derived almost exclusively from experiments and observations using one extant species, the *Se*7942 strain. Therefore, whether Kai proteins functioned as circadian oscillators in ancestral cyanobacteria, or even in extant species other than the *Se*7942 strain, remains unknown.

In this work, we study the function and structure of extant and ancestral Kai-proteins to present a scenario for the evolution of the self-sustained Kai-protein oscillators. According to our estimates, the earliest Kai-protein oscillator emerges in the MRCA of cyanobacteria at approximately 2.2 Ga ago and is able to synchronize with temperature cycles of 18 h, which is shorter than the current rotation period of Earth. The ancient Kai-protein oscillator has been inherited through a long evolutionary process by most extant freshwater cyanobacteria and some marine cyanobacteria living under 24-h environmental cycles.

Results

Feasibility study of reconstructing Kai-protein oscillators in extant species

Duplication of the predecessor of the *kaiC* gene and their subsequent fusion into a double-domain predecessor occurred between 3.8 and 3.5 Ga ago[32]. We used the result of large-scale genome analyses of cyanobacteria and other species[33] to construct a phylogenetic tree of extant double-domain KaiC homologs (Fig. 1a and Supplementary Fig. 1). The KaiC tree included four groups: group I was composed mainly of KaiCs from freshwater cyanobacteria, including *Se*7942 (KaiC^{Se}, ID: 001); group II consisted of marine cyanobacteria; group III included other bacteria; and group IV was formed by other bacteria including archaea. Most freshwater cyanobacteria have only one *kaiC* of group I, but others have additional group III or IV *kaiC* originated from secondary copies or lateral transfer. Thus, these group III and IV KaiCs from freshwater cyanobacteria (gray entries in Fig. 1a) in the protein-based tree can be excluded when identifying groups I–IV and nodes based on species and growing habitant (see Supplementary Discussion).

Rhodobacter sphaeroides KaiC (KaiC^{Rs}, ID: 194), which functions as an hourglass-like timekeeping system[34], and *Rhodopseudomonas palustris* TIE 1 KaiC (KaiC^{Rp}, ID: 184), which is not self-sustained but enhances fitness in the rhythmic environment[35], were classified into group IV in the present KaiC tree. The overall topology and grouping of the protein-based tree of double-domain KaiCs are consistent with those of the 16S rRNA-based phylogenic tree (Supplementary Fig. 2, Supplementary Discussion) as well as with a previous report[32].

We used the in vitro rhythm assay[22] to test the feasibility of establishing the in vitro oscillator for 41 representative extant species including the *Se*7942 strain at pH 8.0 and 30 °C (Supplementary Fig. 3). In most KaiCs from extant species belonging to group I, circadian rhythms were observed in the presence of the corresponding species-specific KaiA and KaiB. For example, *Cyanothece* sp. PCC7822 KaiC (KaiC^{CP}, ID: 007) cycled between phosphorylated and dephosphorylated forms with a period of 27.2 h (Fig. 1b) in the presence of KaiA^{CP} and KaiB^{CP}, as observed in the *Se*7942 system (Supplementary Fig. 3a). The same rhythm was observed in *Oscillatoriales cyanobacterium* JSC 12 KaiC (KaiC^{Os}, ID: 002) (Fig. 1c). Cases in which an obvious rhythm was detected in a set ($A^*B^*C^*$) corresponding to species-specific KaiA (KaiA*), KaiB*, and KaiC* are shown in filled circles in Fig. 1a. Regardless of the behaviors of the $A^*B^*C^*$ set, cases in which oscillation was detected when KaiA* and KaiB* were replaced by KaiA^{Se} and KaiB^{Se}, respectively ($A^{Se}B^{Se}C^*$), are also marked with filled circles in a different column (Fig. 1a). In approximately 80% of group I $A^*B^*C^*$ trials, the rhythm showed a period of 25.2 ± 4.9 h at 30 °C, whereas in approximately 70% of the examined group I $A^{Se}B^{Se}C^*$ sets, the period was 23.4 ± 4.5 h (Supplementary Fig. 3a–c).

In species with KaiCs classified into groups II–IV that did not have a homologous gene for *kaiA*, KaiA^{Se} was hypothetically used for the in vitro rhythm assay ($A^{Se}B^*C^*$). Robust circadian rhythms were observed for most of the examined $A^*B^*C^*$ sets in the first half of the group II entries (approximately 70%, Supplementary Fig. 3d), such as *Synechococcus* sp. RCC307 (KaiC^{SR}, ID: 046) (Fig. 1d) and *Synechococcus* sp. WH 7803 (KaiC^{WH}, ID: 056) (Fig. 1e). In the other half of group II, which consisted of *Prochlorococcus* strains lacking species-specific KaiA, most KaiCs could not be expressed or purified. We were able to purify KaiC from *Prochlorococcus marinus str*. MIT 9211 (ID: 073); however, it showed no rhythm, even in the corresponding $A^{Se}B^{Se}C^*$ set (Fig. 1a and Supplementary Fig. 3d).

Entries in Group III are KaiCs from proteobacteria (cyan entries in Fig. 1a) and bacteria (yellow entries in Fig. 1a), and KaiCs as secondary copies of group I *kaiC* gene (gray entries in Fig. 1a). Proteobacterial KaiC from *Rhodospirillum rubrum* F11 (KaiC^{Rr}, ID: 104) in group III (Fig. 1f) failed to show self-sustained oscillation in their $A^{Se}B^*C^*$ and $A^{Se}B^{Se}C^*$ sets. Two gray entries in Group III, KaiCs from *Cyanothece* sp. ATCC 51142 (KaiC^{Cy2}, ID: 085) and *Synechocystis* sp. PCC 6803 (KaiC^{Sy3}, ID: 093), exhibited self-sustained oscillation in the presence of species-specific KaiB and chimeric KaiA homolog often called KaiA3[36] (Fig. 1g and Supplementary Fig. 3e).

The rhythmic fraction of the group IV entries was relatively low (Fig. 1a): 0% for both the $A^{Se}B^*C^*$ and $A^{Se}B^{Se}C^*$ sets of group IV (Supplementary Fig. 3f). For example, KaiC from *Flavobacterium johnsoniae* UW101 (KaiC^{Fj}, ID: 212) in group IV (Fig. 1h) did not show self-sustained oscillation in either the $A^{Se}B^*C^*$ and $A^{Se}B^{Se}C^*$ sets.

These results suggest that not all extant KaiC homologs with a double-domain architecture have a circadian clock function, which raises the question of how and when KaiC acquired its function as a self-sustained circadian clock.

In vitro reconstruction of ancestral Kai protein oscillators

We restored the possible amino acid sequences of ancestral KaiCs corresponding to seven evolutionary branching points (α–η) (Fig. 1a and Supplementary Fig. 1, Supplementary Discussion). Ancestral KaiCs consist of 509–560 amino acids and contain an N-terminal CI domain and a C-terminal CII domain (Fig. 2a and Supplementary Fig. 4a). Similar to KaiC^{Se}, all ancestral KaiCs retain catalytic glutamates essential for ATPase activity in the CI domain and kinase/phosphatase activity in the CII domain, as well as a potential dual phosphorylation site (S431 and T432 in KaiC^{Se}) in the CII domain (Fig. 2a). A phylogenetic tree of extant KaiB homologs was constructed (Supplementary Fig. 5) and compared with that of the double-domain KaiC homologs (Fig. 1a). According to the similarities in the taxonomic patterns of the belonging species (see coloring by growing habitat), the branches corresponding to the γ, δ, ε, and η points were assigned to the KaiB tree (Supplementary Figs. 5 and 4b), whereas α and β were identified as a point (α/β) with no clear distinction between them. Consistent with a previous study showing that ancestral KaiA appeared at a later time than ancestral KaiB and KaiC[32,37], we were only able to assign three later branches for the γ, δ, and ζ points in our tree of double-domain KaiA homologs (Supplementary Figs. 6 and 4c). Because ancient seawater was neutral (pH ~ 7)[38], whereas the current seawater is slightly basic (pH ~ 8), and because some cyanobacteria undergo a change in intracellular pH in response to the pH of their environment[39], these ancestral forms of Kai proteins were expressed and purified for an in vitro rhythm assay at pH 7.0 and a temperature of 30 °C.

A hypothetical oldest set ($A^{\gamma}B^{\alpha/\beta}C^{\alpha}$) consisting of KaiA$^{\gamma}$, KaiB$^{\alpha/\beta}$, and KaiC$^{\alpha}$ did not show any signs of oscillation, and this was also

https://doi.org/10.1038/s41467-025-59908-7

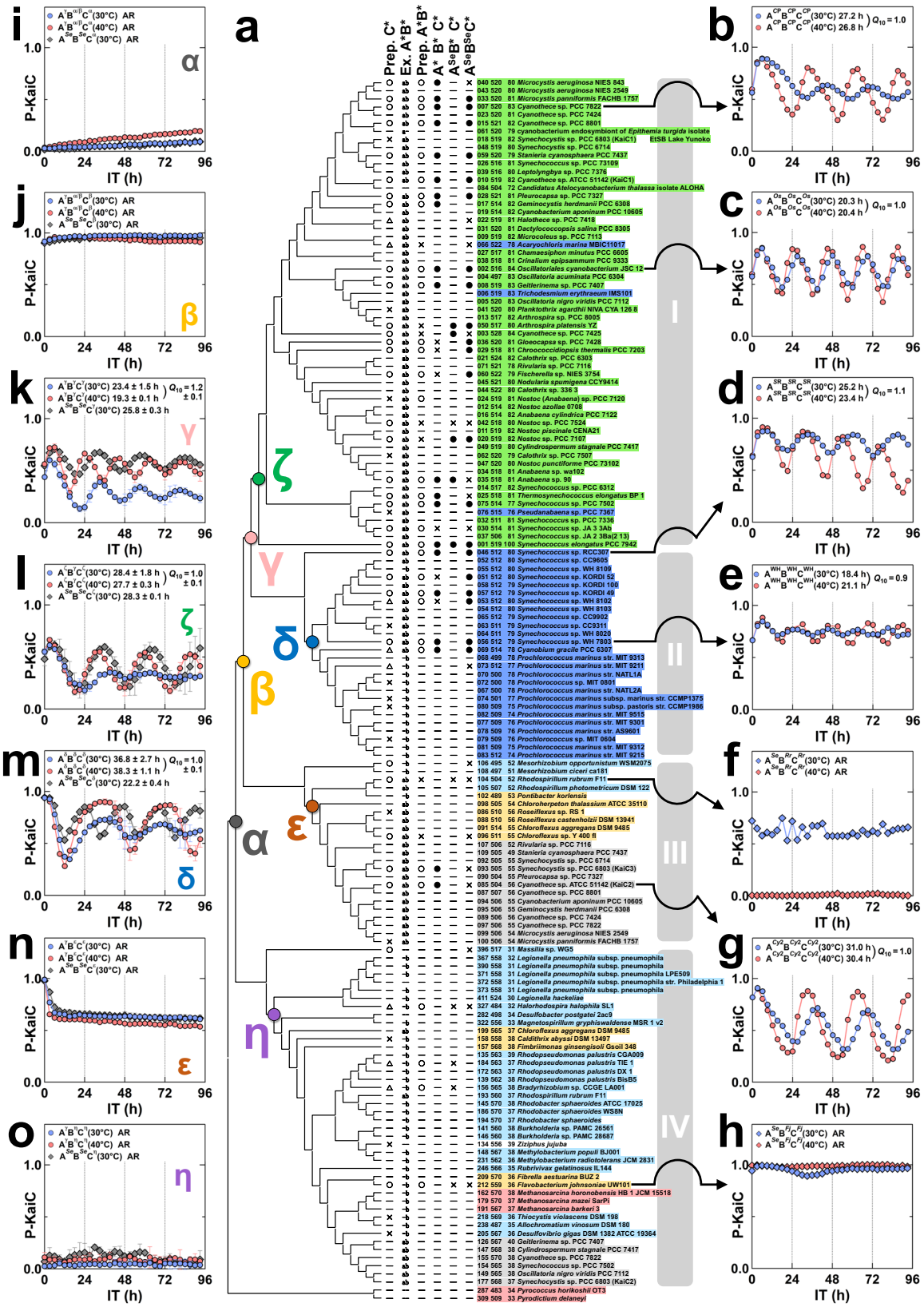

observed in the $A^{Se}B^{Se}C^{\alpha}$ set (Fig. 1i). Similar results were obtained for the second oldest $A^{\gamma}B^{\alpha/\beta}C^{\beta}$ and $A^{Se}B^{Se}C^{\beta}$ sets (Fig. 1j). By contrast, the $A^{\gamma}B^{\gamma}C^{\gamma}$ and $A^{Se}B^{Se}C^{\gamma}$ sets exhibited robust oscillations with periods of 23.4 ± 1.5 and 25.8 ± 0.3 h (Fig. 1k), respectively. Similarly, both the ζ sets ($A^{\zeta}B^{\gamma}C^{\zeta}$: 28.4 ± 1.8 h, $A^{Se}B^{Se}C^{\zeta}$: 28.3 ± 0.1 h, Fig. 1l) and the δ sets ($A^{\delta}B^{\delta}C^{\delta}$: 36.8 ± 2.7 h, $A^{Se}B^{Se}C^{\delta}$: 22.2 ± 0.4 h, Fig. 1m) showed rhythmic oscillation. Neither the ε sets nor the η sets ($A^{\gamma}B^{\varepsilon}C^{\varepsilon}$, $A^{Se}B^{Se}C^{\varepsilon}$, $A^{\gamma}B^{\eta}C^{\eta}$, nor $A^{Se}B^{Se}C^{\eta}$) exhibited any rhythmicity (Fig. 1n, o).

These results indicate that the oldest KaiC$^{\alpha}$ (62% identity to KaiC^{Se}, Fig. 2a) and the subsequent KaiC$^{\beta}$ (74% identity) lacked oscillatory ability and that this ability was acquired during the transition from KaiC$^{\beta}$ to KaiC$^{\gamma}$ (89% identity). Consistent with this interpretation, the

Fig. 1 | Feasibility studies of in vitro oscillators for extant and ancestral Kai proteins. a Phylogenetic tree of extant double-domain KaiC homologs. Cyanobacteria in freshwater, marine cyanobacteria, proteobacteria, bacteria, and euryarchaeota/crenarchaeota are colored green, blue, cyan, yellow, and red, respectively. Group III and IV KaiCs from freshwater cyanobacteria (gray entries) are originated from secondary copies of group I *kaiC* gene or lateral gene transfer. The three numbers preceding the name of each entry indicate the ID number, the total number of amino acids, and the sequence identity with KaiC^{Se}, respectively. A*B*C*: sets of species-specific KaiA*, KaiB*, and KaiC*. A^{Se}B^{Se}C*: sets of KaiA^{Se}, KaiB*, and KaiC*. A^{Se}B^{Se}C*: sets of KaiA^{Se}, KaiB^{Se}, and KaiC*. Rhythmic sets are indicated by filled circles, whereas arhythmic sets are labeled with crosses (see each result in Supplementary Fig. 3). Prep. C* and Prep. A*B* indicate whether species-specific Kai proteins were adequately expressed and purified (open circles), prepared at a level that could be analyzed (triangles), or not prepared at all (crosses). Ex. A*B* indicates the classification of the existence of *kaiA** and *kaiB** genes; e.g., *kaiA** and *kaiB** coexist (ab), only *kaiA** exists (a−), only *kaiB** exists (−b), and neither exists (−). Symbols α–η represent evolutionarily important branching points for which the amino acid sequence of ancestral KaiC was restored (Fig. 2a and Supplementary Fig. 4a). In vitro rhythm assays of A*B*C* (circles) or A^{Se}B*C* (diamonds) at 30 °C (blue) and 40 °C (red) as functions of incubation time (IT) for **b** *Cyanothece* sp. PCC7822 (KaiC^{CP}, ID: 007) in group I, **c** *Oscillatoriales cyanobacterium* JSC 12 (KaiC^{Os}, ID: 002) in group I, **d** *Synechococcus* sp. RCC307 (KaiC^{SR}, ID: 046) in group II, **e** *Synechococcus* sp. WH 7803 (KaiC^{WH}, ID: 056) in group II, **f** *Rhodospirillum rubrum* F11 (KaiC^{Rr}, ID: 104) in group III, **g** *Cyanothece* sp. ATCC 51142 (KaiC^{Cy2}, ID: 085) in group III, and **h** *Flavobacterium johnsoniae* UW101 (KaiC^{Fj}, ID: 212) in group IV. Shown are the representative examples of the fraction of phosphorylated KaiC (P-KaiC) from multiple experiments summarized in Supplementary Fig. 3. AR indicates that the period could not be determined (arrhythmic). In vitro rhythm assays for **i** A$^{\gamma}$B$^{\alpha/\beta}$C$^{\alpha}$ (circles) and A^{Se}B^{Se}C$^{\alpha}$ (diamonds), **j** A$^{\gamma}$B$^{\alpha/\beta}$C$^{\beta}$ (circles) and A^{Se}B^{Se}C$^{\beta}$ (diamonds), **k** A$^{\gamma}$B$^{\gamma}$C$^{\gamma}$ (circles) and A^{Se}B^{Se}C$^{\gamma}$ (diamonds), **l** A$^{\zeta}$B$^{\gamma}$C$^{\zeta}$ (circles) and A^{Se}B^{Se}C$^{\zeta}$ (diamonds), **m** A$^{\delta}$B$^{\delta}$C$^{\delta}$ (circles) and A^{Se}B^{Se}C$^{\delta}$ (diamonds), **n** A$^{\gamma}$B$^{\epsilon}$C$^{\epsilon}$ (circles) and A^{Se}B^{Se}C$^{\epsilon}$ (diamonds), and **o** A$^{\gamma}$B$^{\eta}$C$^{\eta}$ (circles) and A^{Se}B^{Se}C$^{\eta}$ (diamonds). Plots are shown as means ± s.d. of three replicates (see Table 1 for details on the number of replicates and their sources). Blue circles and gray diamonds correspond to the data taken at 30 °C, and red circles correspond to the data taken at 40 °C.

ATPase activities of KaiC$^{\alpha}$ and KaiC$^{\beta}$ were temperature-dependent (Q_{10}: 2.1–2.2), whereas those of KaiC$^{\gamma}$ and KaiC$^{\delta}$ were temperature-compensated (Q_{10}: 0.9–1.2) (Fig. 2b and Supplementary Table 1). Pre–steady-state analysis of the ATPase activity supported this interpretation: KaiC^{Se} exhibits damped oscillation of ATPase activity even in the absence KaiA^{Se} and KaiB^{Se} [29], and similar characteristics were observed in KaiC$^{\gamma}$, KaiC$^{\delta}$, and KaiC$^{\zeta}$ (Fig. 2c). In addition, an *Se*7942 reporter strain in which *kaiC*^{Se} was replaced by *kaiC*$^{\gamma}$ showed a bioluminescent rhythm under constant-light illumination conditions at 30 °C (Fig. 2d, e), and its period length (32.9 ± 0.7 h) was consistent with that of the in vitro A$^{\gamma}$B$^{\gamma}$C$^{\gamma}$ set at pH 7.6–7.8 and 30 °C (Fig. 2f). The acquisition of oscillatory abilities that occurred in the transformation from KaiC$^{\beta}$ to KaiC$^{\gamma}$ is not a wild hypothesis confined to the test tube but a possible evolutionary event that could have occurred in primitive cyanobacteria.

We found that the period length of the A$^{\gamma}$B$^{\gamma}$C$^{\gamma}$ set was sensitive to ambient pH. The cycle length, which was 39 h at pH 8.0 and 30 °C, became shorter under acidic conditions, finally stabilizing at 23.4 ± 1.5 h at pH 7.0 and 30 °C (Fig. 2f). The A^{Se}B^{Se}C^{Se} and A$^{\delta}$B$^{\delta}$C$^{\delta}$ sets showed a similar tendency, although they were less pH-dependent than the A$^{\gamma}$B$^{\gamma}$C$^{\gamma}$ set. The results for the A^{Se}B^{Se}C$^{\gamma}$ set (Figs. 1k and 2f) suggest that the pronounced pH sensitivity of the period length is derived from KaiC$^{\gamma}$ itself. Taking into account that the intracellular pH of cyanobacteria changes in response to the external pH[39], that the pH of ancient seawater was ~7[38], and that the period length is insensitive to ionic strength (Supplementary Fig. 7), the period length at pH 7.0 and 30 °C is reasonably concluded to be a better estimate for ancestral types than that at pH 8.0 and 30 °C. In fact, the A$^{\gamma}$B$^{\gamma}$C$^{\gamma}$ set was entrained by external temperature cycles of 18 to 24 h at pH 7 (Fig. 3a). It worth noting that successful entrainment by the short 18-h cycle was confirmed only for the γ set at pH 7 (Fig. 3a), but not for the A^{Se}B^{Se}C^{Se} set at pH 8 (Fig. 3b)[40].

Structural evolution of ancestral KaiC

To explore the structural origin of the autonomous oscillatory properties acquired in the transition from β to γ, we solved the X-ray crystal structures for KaiC$^{\beta}$, KaiC$^{\gamma}$, and KaiC$^{\delta}$ (Supplementary Table 2). The overall structures of KaiC$^{\gamma}$ and KaiC$^{\delta}$ were similar to that of KaiC^{Se} (Fig. 4a), and their main chains could be superimposed with a root-mean-squared deviation (RMSD) of 1.1 Å. The similarity between KaiC$^{\gamma}$ and KaiC^{Se} was confirmed by the superimposition of other parts using one particular CII domain (star in Fig. 4b). By contrast, the structure of KaiC$^{\beta}$ differed markedly from that of KaiC$^{\gamma}$ (main-chain RMSD of 2.0 Å). When KaiC$^{\beta}$ and KaiC$^{\gamma}$ were superimposed using one of the CII domains (star in Fig. 4c), the other CI and CII domains did not overlap (main-chain RMSD of 5.3 Å). These findings suggest that ancestral KaiCs acquired the basic architecture for establishing the autonomous oscillator found in KaiC^{Se} during the transition from KaiC$^{\beta}$ to KaiC$^{\gamma}$.

Structural differences between KaiC$^{\beta}$ and KaiC$^{\gamma}$ were found in both the CI and CII domains. Three major differences were observed in the CI domain with the ATPase activity responsible for period-length determination[29,30]. The first is the type of bound nucleotide. KaiC$^{\gamma}$ and KaiC$^{\delta}$ were crystallized in the pre-hydrolysis state with a non-hydrolyzable ATP analog (AMP-PNP) bound to the CI domain, as described for KaiC^{Se} [29,41] (left in Fig. 4d and Supplementary Fig. 8a); by contrast, KaiC$^{\beta}$ was crystallized in the post-hydrolysis state with an adenosine diphosphate (ADP) bound to its CI active site even in the presence of 5 mM AMP–PNP (right in Fig. 4d and Supplementary Fig. 8b).

The second difference is the interface between two adjacent CI domains. In the pre-hydrolysis states of KaiC$^{\gamma}$, KaiC$^{\delta}$, and KaiC^{Se} (left in Fig. 4d and Supplementary Fig. 8c), each CI–CI interface is stabilized by the hydrogen bond between the Ser residue side chain (S46$^{\gamma}$, S44$^{\delta}$, and S48^{Se}: Fig. 2a) in one CI domain and the carboxyl oxygen atom of the Glu residue (E196$^{\gamma}$, E194$^{\delta}$, and E198^{Se}) in the adjacent domain. However, in KaiC$^{\beta}$, the corresponding Ser residue is replaced by Pro (P42$^{\beta}$: Fig. 2a) and the packing of the CI–CI interface becomes loose because of the cleavage of the inter-domain hydrogen bond (right in Fig. 4d), as observed for the post-hydrolysis CI ring of KaiC^{Se} [27,29]. In addition, the replacement of the amino acid corresponding to S199 in KaiC$^{\gamma}$ (S199$^{\gamma}$) by A195 in KaiC$^{\beta}$ (A195$^{\beta}$) leads to further selective stabilization of the post-hydrolysis CI conformation of KaiC$^{\beta}$. In the pre-hydrolysis state of KaiC$^{\gamma}$ (left in Fig. 4d), the α_8 helix is stabilized by the hydrogen bond between S199$^{\gamma}$ and E195$^{\gamma}$ (between S197$^{\delta}$ and E193$^{\delta}$ in KaiC$^{\delta}$, and between S201^{Se} and E197^{Se} in KaiC^{Se}). In KaiC$^{\beta}$, however, cleavage of this hydrogen bond by A195$^{\beta}$ enables the partial unfolding of the α_8 helix (right in Fig. 4d), as confirmed by the loose CI–CI interface of the post-hydrolysis CI of KaiC^{Se}[27,29]. These observations support the preferential binding of ADP to the loose CI–CI interface of KaiC$^{\beta}$.

The third difference is the insertion of a residue into the loop enclosing the nucleotide bound in the active site of the CI domain. Compared with KaiC^{Se} and KaiC$^{\gamma}$ (top in Fig. 4e), KaiC$^{\beta}$ had a proline residue inserted at the 235th position (P235$^{\beta}$: Fig. 2a) and its structure showed that the residue was located in the turn of the nucleotide enclosure loop (bottom of Fig. 4e). The distorted structure of the ADP bound nearby suggests that, in KaiC$^{\beta}$, P235$^{\beta}$ pushes its adenine ring toward the center of the CI ring and inhibits the release of bound ADP. In rhythmic KaiCs such as KaiC$^{\gamma}$, KaiC$^{\delta}$, and KaiC^{Se}, no such inhibitory structures for releasing nucleotides exist. Consistent with this structural observation, biochemical experiments showed that ADP bound to KaiC$^{\beta}$ was highly stabilized and, in contrast to ADP bound to KaiC^{Se} and KaiC$^{\gamma}$, was not easily exchanged by AMP–PNP (Fig. 4f).

https://doi.org/10.1038/s41467-025-59908-7

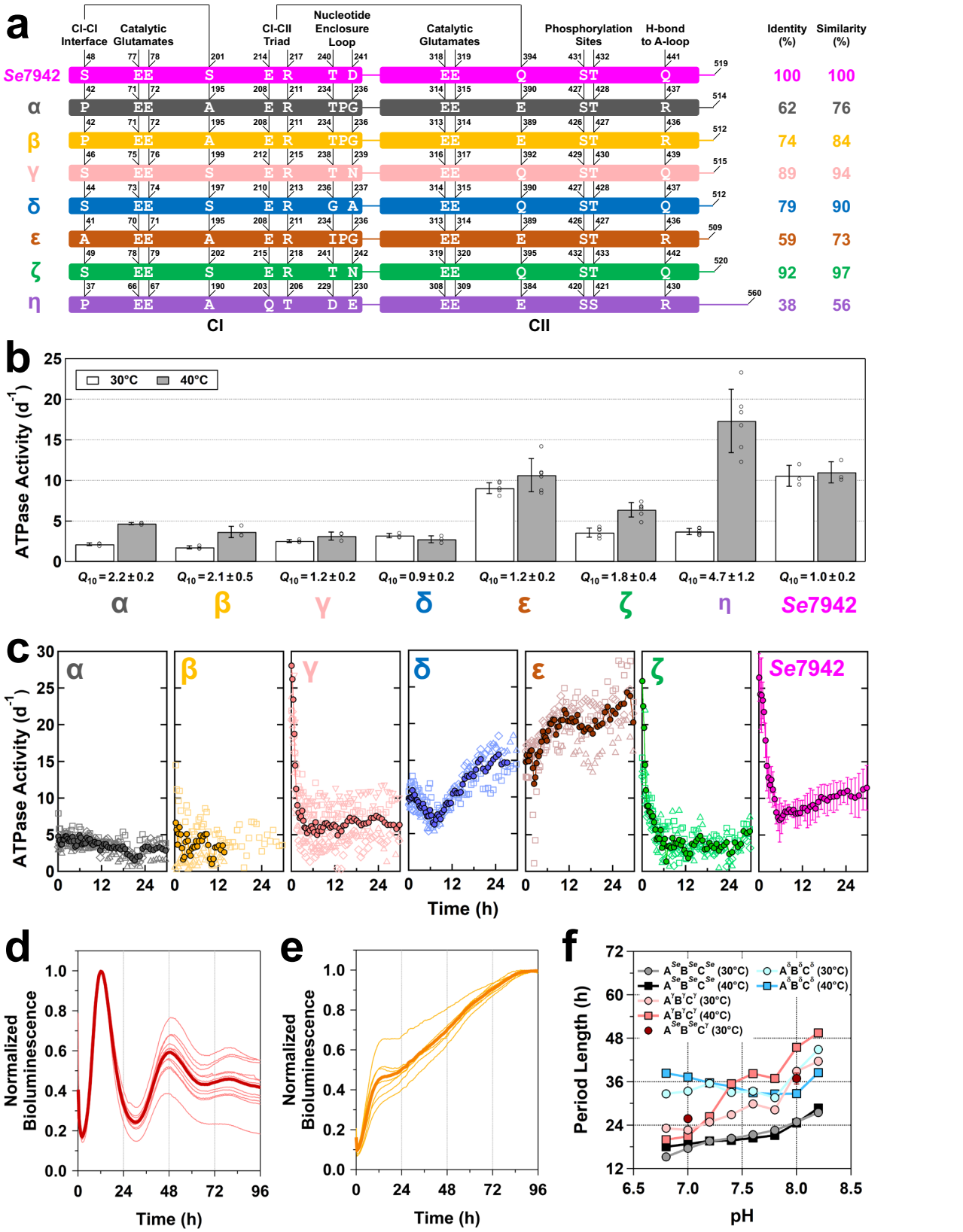

These observations suggest that the loose CI–CI interface results in the preferential binding of ADP (right in Fig. 4d) and that the elongation of the nucleotide enclosure loop (bottom in Fig. 4e) further prevents the exchange of generated or bound ADP (Fig. 4f). These factors might have caused the consistent occupation of the CI site by ADP in KaiC$^{\beta}$, resulting in a reduction of the ATPase activity (1.8 ± 0.2 ATP d^{-1} at 30 °C, Fig. 2b) and the loss of the damped oscillatory relaxation in KaiC$^{\beta}$ (Fig. 2c). KaiC might have acquired its oscillatory ability by evolving its CI structure to enable nucleotides bound to the CI domain to be exchanged on a reasonable circadian time scale.

The structural differences between KaiC$^{\beta}$ and KaiC$^{\gamma}$ were not only observed in the CI–CI interface but also in the CII domain and the

https://doi.org/10.1038/s41467-025-59908-7

Fig. 2 | Domain architecture and biochemical properties of ancestral KaiCs. **a** Key residues and motifs mapped to the domain compositions of KaiC^{Se} and ancestral KaiCs. **b** Temperature dependence of the steady-state ATPase activity of ancestral KaiCs at pH 7.0 and KaiC^{Se} at pH 8.0. Open circles correspond to raw data shown in Supplementary Table. 1. Bar graphs show means ± s.d.; For KaiC^{Se} (30 °C and 40 °C), three independent purifications; For KaiC$^{\alpha}$, KaiC$^{\beta}$, and KaiC$^{\delta}$ (30 °C and 40 °C), three replicates from a single purification; For KaiC$^{\gamma}$, three replicates from a single purification (30 °C) and three replicates from two independent purifications (40 °C); For KaiC$^{\varepsilon}$ and KaiC$^{\eta}$ (30 and 40 °C), six replicates from two independent purifications; For KaiC$^{\zeta}$, six replicates from a single purification (30 °C) and six replicates from two independent purifications (40 °C). **c** Pre−steady-state analysis of the ATPase activity. Dark-colored circles correspond to the mean of separate experiments; For KaiC$^{\alpha}$, KaiC$^{\delta}$, KaiC$^{\varepsilon}$, and KaiC$^{\zeta}$, three independent purifications (open squares, triangles, and diamonds); For KaiC$^{\beta}$, two independent purifications (open squares and triangles); For KaiC$^{\gamma}$, four independent purifications (open squares, triangles, inverted triangles, and diamonds). The data of KaiC^{Se} were taken from the previous report[29] and presented as mean ± s.d. of separate experiments using three independent purifications. Bioluminescent rhythm assays for *Se*7942 reporter strains carrying **d** *kaiA*^{Se}: *kaiB*^{Se}: *kaiC*$^{\gamma}$ and **e** *kaiA*^{Se}: *kaiB*^{Se}: *kaiC*$^{\beta}$, but without *kaiC*^{Se}, were performed under continuous-light illumination condition at 30 °C. Thin and thick lines represent individual ($n = 12$ and 7 for (**d**) and (**e**), respectively) and average traces, respectively. The period length (32.9 ± 0.7 h) of the strain with *kaiA*^{Se}: *kaiB*^{Se}: *kaiC*$^{\gamma}$ was consistent with that of the in vitro A$^{\gamma}$B$^{\gamma}$C$^{\gamma}$ set at pH 7.6–7.8 at 30 °C in (**f**). **f** pH-dependence of the period length for the in vitro A$^{\gamma}$B$^{\gamma}$C$^{\gamma}$, A$^{\delta}$B$^{\delta}$C$^{\delta}$, and A^{Se}B^{Se}C^{Se} sets at 30 °C and 40 °C. The data for the A^{Se}B^{Se}C$^{\gamma}$ set at 30 °C at pH 7.0 (three replicates from a single purification) and pH 8.0 (three independent purifications) were presented by brown circles as means ± s.d. Each plot other than the A^{Se}B^{Se}C$^{\gamma}$ set corresponds to a single experiment using a single purification.

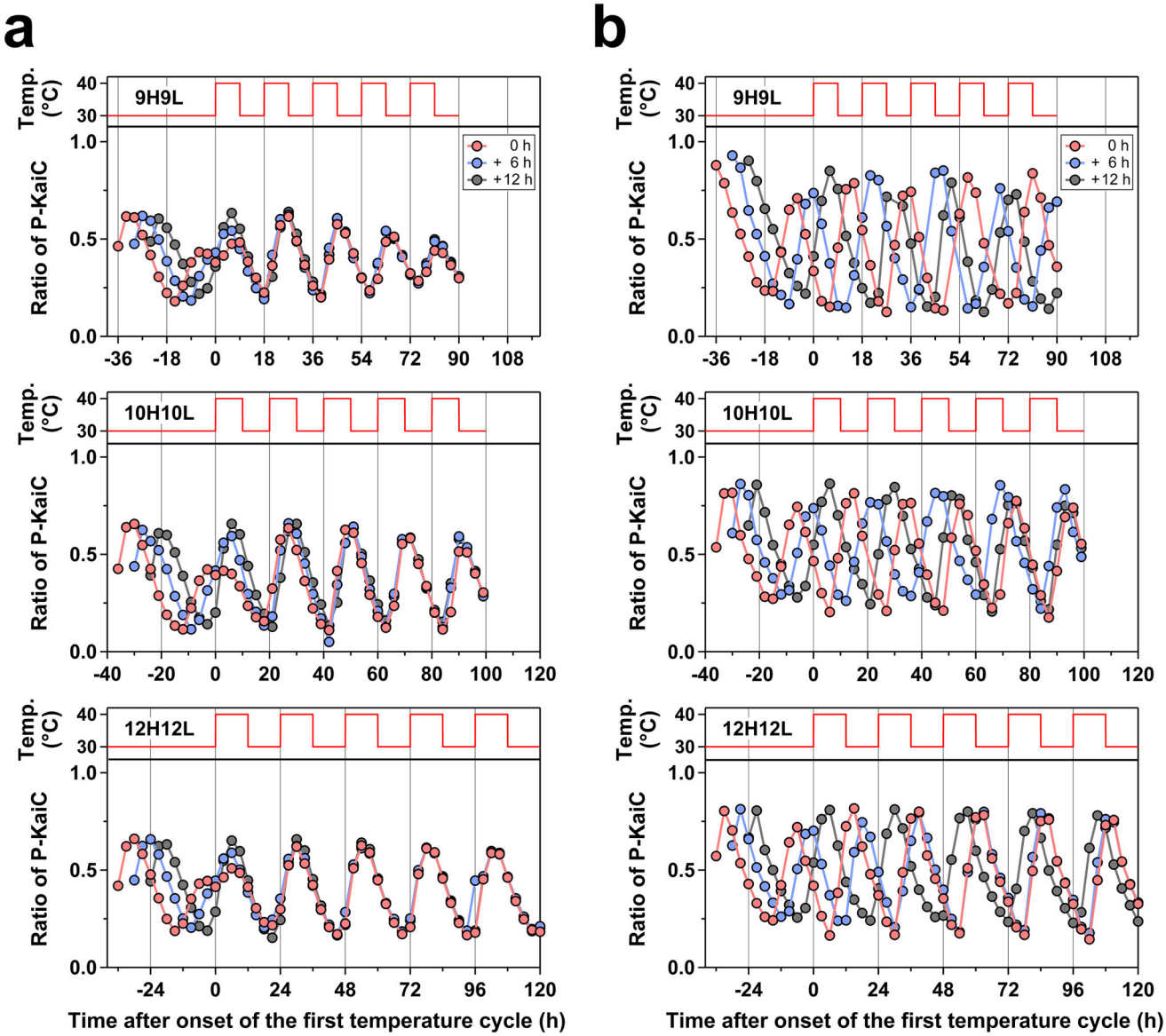

Fig. 3 | In vitro temperature entrainment of the Kai-protein oscillators. **a** Fraction of phosphorylated KaiC (P-KaiC) of the A$^{\gamma}$B$^{\gamma}$C$^{\gamma}$ set at pH 7.0. **b** P-KaiC of the A^{Se}B^{Se}C^{Se} set at pH 8.0. Each set was reconstituted at 0 h (red circles), 6 h (blue circles), and 12 h (gray circles) intervals and incubated at 30 °C for 36, 30, and 24 h, respectively. After incubation, the pre-incubated samples were exposed to temperature cycles (red lines) of 9 h at 40 °C and 9 h at 30 °C (9H9L: top), 10 h at 40 °C and 10 h at 30 °C (10H10L: middle), or 12 h at 40 °C and 12 h at 30 °C (12H12L: bottom).

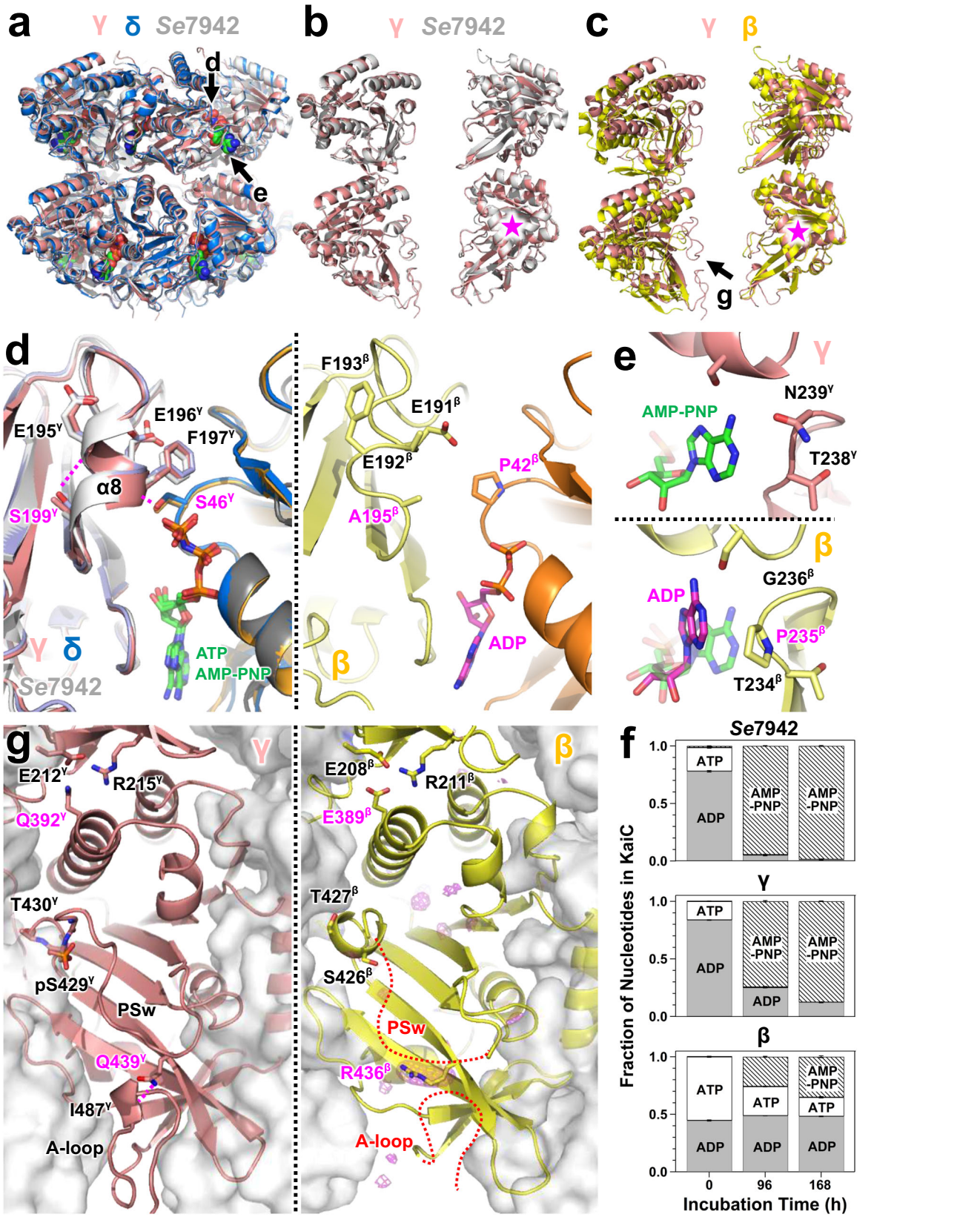

CI–CII interface. In rhythmic KaiC$^{\gamma}$, a region upstream of the C-terminal tail to which KaiA$^{\gamma}$ binds[42] was clearly resolved as a loop structure (A-loop) with a stabilizing hydrogen bond between Q439$^{\gamma}$ and I487$^{\gamma}$ (left in Fig. 4g), as observed between Q441^{Se} and I489^{Se} in KaiC^{Se} [41,43]. In KaiC$^{\beta}$, however, the A-loop was destabilized by R436$^{\beta}$, which breaks this hydrogen bond (right in Fig. 4g). The electron density of the phosphor-switch, which changes conformation upon phosphoryl modification of the dual phosphorylation site (S431^{Se} and T432^{Se}) in rhythmic KaiC^{Se} [41], was clearly identified in KaiC$^{\gamma}$ but not in KaiC$^{\beta}$ (right in Fig. 4g). In addition, the 389th residue located in the CI–CII interface is Glu in KaiC$^{\beta}$ (E389$^{\beta}$), whereas the corresponding residue is Gln in the rhythmic KaiC$^{\gamma}$ (Q392$^{\gamma}$) and KaiC^{Se} (Q394^{Se}). In KaiC^{Se}, Q394^{Se} is critical

Fig. 4 | Crystal structures of ancestral KaiCs. a Similarity of the overall structures of KaiC$^{\gamma}$ (pink), KaiC$^{\delta}$ (blue), and KaiC^{Se} (gray, PDB ID: 7DXQ). Black thick arrows indicate the viewing directions for each panel. **b** Superimposition of KaiC$^{\gamma}$ (pink) and KaiC^{Se} (gray) using one of the CII domains (magenta star). The main-chain root-mean-squared deviation (RMSD) values of the fitted and other parts were 0.7 and 1.2 Å, respectively. For clarity, only the two most distantly located subunits within the hexamer are shown. **c** Superimposition of KaiC$^{\gamma}$ (pink) and KaiC$^{\beta}$ (yellow) using one of the CII domains (magenta star). Main-chain RMSD values of the fitted and other parts were 0.7 and 5.3 Å, respectively. **d** Zoomed-in views of the pre-hydrolysis CI–CI interfaces (left) for KaiC$^{\gamma}$ (pink/orange), KaiC$^{\delta}$ (cyan/blue), and KaiC^{Se} (white/gray), and the post-hydrolysis CI–CI interface (right) for KaiC$^{\beta}$ (yellow/brown). Dotted magenta lines represent hydrogen bonds. **e** Zoomed-in views of the nucleotide enclosure loop for KaiC$^{\gamma}$ (top) and KaiC$^{\beta}$ (bottom). In bottom panel, KaiC$^{\gamma}$ was superimposed on KaiC$^{\beta}$ using one CI protomer, and then only the AMP–PNP molecule (green stick model) bound to KaiC$^{\gamma}$ is shown for comparison with the ADP molecule (magenta stick model) of KaiC$^{\beta}$. **f** Exchange with AMP–PNP was barely detected in KaiC$^{\beta}$-bound ADP, in contrast to KaiC^{Se}- and KaiC$^{\gamma}$-bound ADP. Ancestral KaiCs and KaiC^{Se} were incubated at pH 7.0 and 8.0, respectively, at 30 °C in the presence of 1 mM AMP–PNP; the fractions of nucleotides bound by KaiCs were quantified. Bar graphs show mean ± s.d. of three replicates from a single purification. **g** CII domains of KaiC$^{\gamma}$ (left) and KaiC$^{\beta}$ (right) viewed from the inner-diameter side of the hexamers. A-loop and PSw correspond to the C-terminal tail and the phosphor-switch, respectively, in KaiC. The magenta meshes represent the F_{obs}–F_{calc} omit maps contoured at 3σ. Dotted red lines represent potentially flexible parts that could not be determined because of poor electron density.

for establishing the rhythmic coupling between the CI and CII domains by switching the interaction with E214^{Se} and/or R217^{Se} (Fig. 2a and left in Fig. 4g), as evidenced by the arrhythmicity of the Q394E variant of KaiC^{Se} [41].

Discussion

Conservation of autonomous Kai-protein oscillators in group I

Since the successful in vitro reconstruction of the A^{Se}B^{Se}C^{Se} oscillator in 2005[22], the *Se*7942 strain has become the major target of research on the circadian clock system in cyanobacteria[20,21]. So far, there have been no reports of comprehensive feasibility study of establishing in vitro oscillators for bacteria other than the *Se*7942 strain. For this reason, it was possible to argue that many cyanobacteria actually require transcription-translation feedback[44] to maintain their rhythm, and that *Se*7942 is an exceptional case. The present study clearly demonstrates that this is not the case, and that the self-sustained Kai-protein oscillators are conserved in approximately 80% of group I cyanobacteria (Fig. 1a).

At the same time, careful interpretation may be needed for the other entries of group I, which cannot be tested due to unavailability of the Kai-protein samples or failed to show the self-sustained circadian oscillation in vitro (Fig. 1 and Supplementary Fig. 3a–c). For example, it is known that *Nostoc* (*Anabaena*) sp. PCC 7120 exhibits in vivo bioluminescence rhythm[45,46], but in this study, we could not conduct the in vitro test because its species-specific KaiC^{No} (ID: 024 in Fig. 1a) was not expressed even by 12 different trials using different expression hosts, fusion tags, and culturing conditions[47]. Since KaiC from *Anabaena* sp. 90 (KaiC^{An}, ID: 035 in Fig. 1a) was rhythmic in vitro in the presence of KaiA^{An} and KaiB^{An} (Supplementary Fig. 3b), it is possible that the A^{No}B^{No}C^{No} set will also be judged as rhythmic if KaiC^{No} can be prepared. As another example, KaiC from *Fischerella* sp. NIES 3754 (KaiC^{Fi}, ID: 060 in Fig. 1a) showed circadian rhythm in the presence of KaiA^{Se} and KaiB^{Se}, but was determined to be arrhythmic in the presence of KaiA^{Fi} and KaiB^{Fi} (Supplementary Fig. 3c). One possible explanation for these examples is that a part of the A*B*C* sets in group I becomes stabilized and self-sustained only in special intracellular circumstances that cannot always be fully reproduced in vitro. If we were allowed to take such an extended view of self-sustained protein-based oscillation, the proportion of group I entries with the autonomous Kai-protein oscillators would be even higher than 80%. In this context, although this study does not deny the self-sustainment in the extended sense for the α and β sets in ancient bacteria, but it is clear from our experiments that they are not self-sustained in vitro in the strict sense.

γ node as the time when self-sustained Kai protein oscillators were established

It is important to verify obtained results from the perspective of uncertainties associated with the sequence estimation. The uncertainty in sequence prediction may come from the arbitrary nature of how much gap is allowed when aligning sequences of existing species. We thus performed the same in vitro rhythm assay on another set of ancestral sequences, which was estimated from the alignment using different gap-opening penalty (Supplementary Fig. 9a–c). While both the α and β nodes were arrhythmic, the γ nodes were found to be rhythmic regardless of the way of the sequence prediction (Supplementary Fig. 9d–f). Furthermore, the ancestral lineage of the autonomous oscillations originating from the γ node provides a reasonable explanation for the distribution pattern of the Kai-protein autonomous oscillators in the extant species (groups I–IV), excluding entries derived from secondary copies or lateral transfer (gray entries in Fig. 1a). These evidences suggest the limited effects of the arbitrariness of the sequence estimation on the present view that the self-sustained Kai-protein oscillator appeared at the γ node.

On the other hand, the effects of the uncertainty on the estimation of the cycle length may not be negligible for the following three reasons. First, the length of the cycle is a characteristic of the system composed of three types of ancestral Kai proteins, so the uncertainty is at least potentially additive. Second, the period length of the A^{Se}B^{Se}C^{Se} set can be tuned in the range of 60% to 660% even by one amino acid substitution in a very critical region of KaiC^{Se} [48]. Third, the cycle length of the A$^{\gamma}$B$^{\gamma}$C$^{\gamma}$ set was more pH-sensitive than that of the A^{Se}B^{Se}C^{Se} set (Fig. 2f). Taken together, it would be reasonable to conclude that there is uncertainty between the period length of the reconstructed ancestral systems and the true period length of ancient bacteria.

A possible scenario for the evolution of the Kai protein oscillator

The 16S rRNA-based phylogenic tree (Supplementary Fig. 2) shows the presence of a node (γ point) diverging into freshwater and marine cyanobacteria, which can be interpreted as corresponding to the MRCA of cyanobacteria. KaiC$^{\gamma}$ is the topologically identical node that branches into the extant KaiCs of freshwater cyanobacteria (group I) and marine cyanobacteria (group II) (Fig. 1a and Supplementary Fig. 1), and the same applies to KaiB$^{\gamma}$ (Supplementary Fig. 5) and KaiA$^{\gamma}$ (Supplementary Fig. 6). These observations clearly indicate that the A$^{\gamma}$B$^{\gamma}$C$^{\gamma}$ set functioned as the self-sustained circadian oscillator in the MRCA of cyanobacteria capable of oxygenic photosynthesis.

There are many estimates as to when the cyanobacterial MRCA first appeared[2], which range from 3.5 Ga to 1.5 Ga ago[1,3–6]. Our estimate obtained using 16S rRNA sequences dated an ancestral bacterium at an α/β point at 3.1 (3.5–2.8: upper–lower confidence intervals) Ga ago and the MRCA of cyanobacteria at the γ point at 2.2 (2.8–1.7) Ga ago (Fig. 5 and Supplementary Table 3). An ancestral form of the double-domain KaiA, which is evolutionarily related to KaiA$^{\gamma}$, might have appeared approximately 1.0 Ga ago[32]; however, its appearance was subsequently updated to an earlier period, as late as 1.5 Ga ago[37].

Under our divergence time estimate, the MRCA of cyanobacteria would have emerged around the GOE and first SEE period (Fig. 5). This period is characterized by the enhancement of oxygenic photosynthesis due to changes in the properties of ancient cyanobacteria[1–3] or other ancient bacteria[4–6], which destroyed the methane greenhouse and triggered global glaciation[49]. The resonance between the endogenous clock and environmental light–dark cycles is the basis for more

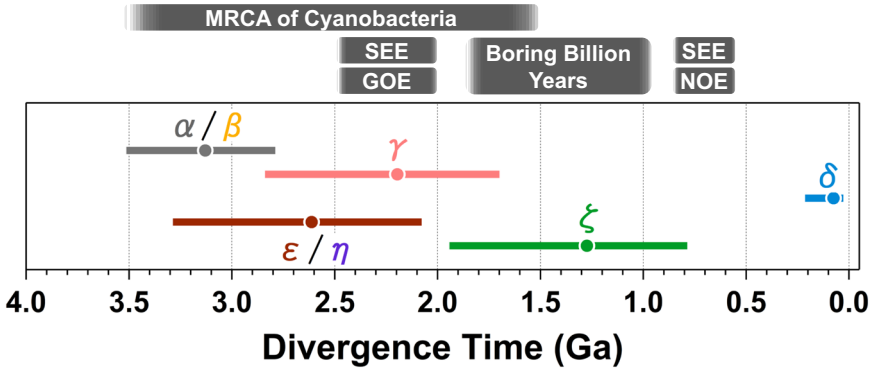

Fig. 5 | Evolutionary origins and diversification of self-sustained Kai protein circadian oscillators. Divergence times were estimated on the basis of TimeTree[53] analysis using 16S rRNA sequences. Filled circles and horizontal bars indicate estimated divergence times (1 Ga = 1 billion years) and confidence intervals, respectively (Supplementary Table 3). The approximate times of the emergence of the most recent common ancestor (MRCA) of cyanobacteria[1–6], Great Oxidation Event (GOE)[7], first and second Snowball Earth events (SEEs)[8–10], the post-GOE period known as the "boring billion years" of ever-stable global conditions[64], and the Neoproterozoic Oxygenation Event (NOE)[11,12] are schematically shown for reference.

efficient growth and survival of organisms, including cyanobacteria[50]. Thus, it is reasonable to speculate that the acquisition of the autonomous γ set allowed the MRCA of cyanobacteria to expect the timing of the next sunrise and prepare in advance to initiate oxygenic photosynthesis accordingly. The Earth's rotation period 2 Ga ago has been suggested to be approximately 4 h shorter than that at present[14]; however, depending on the pH of the growing environment, the γ set in the cyanobacterial MRCA might have been sufficiently functional as a circadian oscillator (Figs. 1k and 3).

Regardless of the accuracy of the divergence time estimation, another ancestral bacterium corresponding to the ε/η point appeared at approximately the same time as the MRCA of cyanobacteria (Fig. 5). The ε/η point is assumed to possess not–self-sustained (Fig. 1o) and temperature-dependent (Fig. 2b) KaiC$^{\eta}$, an ancestral form of the hourglass-like KaiC^{Rs} [34] and not–self-sustained KaiC^{Rp} [35]. The self-sustained protein-based circadian oscillator established in the γ set was subsequently inherited by KaiC$^{\zeta}$ and KaiC^{Se} and, consequently, by approximately 70% of group I cyanobacteria in freshwater (Fig. 1a and Supplementary Fig. 1). The inheritance from KaiC$^{\gamma}$ applied not only to KaiC$^{\zeta}$ but also to KaiC$^{\delta}$, and the autonomous oscillatory property was eventually passed on to marine cyanobacteria located downstream of KaiC$^{\delta}$. However, our results indicate that it was not inherited by the *Prochlorococcus* group located downstream of KaiC$^{\delta}$ or that the inherited traits have changed by today. Given that the molecular evolution of oxygenic photosynthesis pre-dates the cyanobacterial MRCA by >1 Ga[2,4], the unique evolution of the ancestral Kai proteins during the emergence of the cyanobacterial MRCA provided the autotrophic basis for the time-optimal acquisition and consumption of energy, later leading to their massive proliferation across various habitats on Earth.

Methods

Construction of protein-based phylogenic trees

The amino acid sequences of KaiC homologs were obtained from a dataset described previously[33]. From a total of 1194 entries, duplicate entries that had identical sequences but were from different species/strains were removed, resulting in 151 entries of 480–570 amino acid residues with >30% sequence identity to KaiC^{Se}. These were extracted to form a dataset for analyzing KaiC homologs with double-domain structures (Supplementary Fig. 1).

The MEGA X software (version 10.1.7)[51] was used for phylogenic analyses. The 151 sequences were arranged using pairwise/multiple alignments with a gap-opening penalty of 7.5. A preliminary phylogenetic tree was constructed using the maximum likelihood method, and 100 bootstrap replications were generated. To confirm the stability of the resultant phylogenetic pattern, different alignment results were analyzed using gap-opening penalties of 2.5, 5.0, 10.0, 15.0, and 20.0. In the preliminary phylogenetic trees, double-domain homologs of KaiC were classified into four groups as follows: cyanobacteria in freshwater (group I: 58 entries), cyanobacteria in seawater (group II: 26 entries), other bacteria (group III: 23 entries), other bacteria including archaea (group IV: 42 entries), and outgroup (2 entries). The final phylogenetic tree of double-domain KaiC homologs (Fig. 1a) was obtained using a gap-opening penalty of 7.5 through 500 bootstrap replications. A detailed description of the entries in each group is provided in Supplementary Discussion and Supplementary Fig. 1.

Phylogenetic analyses of KaiA and KaiB homologs were performed as described for KaiC using a dataset from a previous study[33]. For KaiB, we extracted 193 entries of 80–120 amino acid residues with >30% sequence identity to KaiB^{Se} (Supplementary Fig. 5). For KaiA, extraction was performed with 50–350 amino acid residues with >30% sequence identity to KaiA^{Se}, resulting in 151 entries of double-domain homologs of KaiA (Supplementary Fig. 6). The species used to construct the phylogenetic trees for KaiA and KaiB were not necessarily identical to those used for the KaiC tree. The final phylogenetic trees for KaiB (Supplementary Fig. 5) and KaiA (Supplementary Fig. 6) were obtained using a gap-opening penalty of 7.5 through 500 bootstrap replications. See Supplementary Information for detailed descriptions of the entries in each group.

Construction of 16S rRNA-based phylogenic trees

The 16S rRNA sequences of extant species with double-domain KaiC homologs were obtained from KEGG[52]. The 16S rRNA-based tree shown in Supplementary Fig. 2 was constructed using MEGA X software (version 10.1.7) with 108 entries of the 151 KaiC homologs used for construction of the protein-based tree (Fig. 1a).

Restoration of amino acid sequences of ancestral KaiCs

The amino acid sequences corresponding to seven nodes on the phylogenic tree of KaiC (Fig. 1a) were inferred on the basis of the maximum likelihood estimation using the amino acid substitution model of LG with Freqs. (+F) and gamma-distributed substitution rates. The oldest ancestor (KaiC$^{\alpha}$) was detected directly below a node branching into groups I–IV, *Pyrococcus horikoshii* OT3 KaiC (KaiC^{Hori}), and *Pyrodictium delaneyi* KaiC (KaiC^{Dela}).

There were two branches emerging from KaiC$^{\alpha}$: one ended in groups I–III, and the other ended in group IV. A node connecting to groups I–III (KaiC$^{\beta}$) showed high bootstrap values (98%–99%) irrespective of the gap-opening penalties (7.5–15). The KaiC$^{\beta}$ node branched into groups I–II and group III. A node branching into groups I and II (KaiC$^{\gamma}$) also emerged with high bootstrap values (99%) irrespective of the gap-opening penalties used. Although the common ancestor of group II (KaiC$^{\delta}$) showed a high bootstrap value (31%–97%), those of group I (KaiC$^{\zeta}$) and group III (KaiC$^{\varepsilon}$) showed relatively lower values (20%–51% and 53%–63%, respectively). The common ancestor of group IV (KaiC$^{\eta}$) was detected with the bootstrap vale (98%) as high as those of KaiC$^{\beta}$ and KaiC$^{\gamma}$.

Restoration of amino acid sequences of ancestral KaiAs and KaiBs

The amino acid sequences corresponding to the nodes on the phylogenic trees of KaiA and KaiB were estimated as described for ancestral KaiCs. In the KaiB tree constructed with 193 entries (Supplementary Fig. 5), we assigned one node for each, KaiB$^{\gamma}$ and KaiB$^{\delta}$, on the basis of similarities in the taxonomic patterns of the corresponding entries (see coloring by growth habitat in Supplementary Figs. 1 and 5). The KaiB$^{\delta}$ node was located downstream of KaiB$^{\gamma}$. Because a node upstream of KaiB$^{\gamma}$ was a common ancestor for all entries, it was termed KaiB$^{\alpha/\beta}$. A node that did not contain downstream archaeal entries was termed KaiB$^{\varepsilon}$.

Only three later branching points (γ, δ, and ζ) could be assigned in the double-domain KaiA tree consisting of 151 entries (Supplementary Fig. 6), which is consistent with the later appearance of ancestral KaiA than ancestral KaiB[37]. KaiA$^{\gamma}$ was reasonably allocated to a node corresponding to a common ancestor of the double-domain KaiA from both freshwater cyanobacteria and seawater cyanobacteria. Similarly, KaiA$^{\zeta}$ and KaiA$^{\delta}$ were assigned to nodes corresponding to ancestors of cyanobacteria in freshwater and seawater, respectively.

Divergence time estimation

The divergence times of the α/β, γ, δ, ε/η and ζ points in the 16S rRNA-based tree (Supplementary Fig. 2) were estimated using MEGA X software (version 10.1.7)[51]. According to the TimeTree[53] estimate of the divergence time between *Synechococcus* and *Flavobacterium*, a calibration point was established at the α/β point as normal distribution with a median at 3.134 Ga and a deviation of 0.5 Ga.

Cloning of extant and ancestral *kaiA*, *kaiB*, and *kaiC*

The DNA sequences of extant and ancestral Kai-proteins were synthesized by Eurofins genomics with codon optimization for expression in *Escherichia coli* (*E. coli*). Unless otherwise stated, the synthesized genes were cloned into the pGEX6P-1 vector (Cytiva) with BamHI and NotI cleaving sites to overexpress GST-tagged Kai proteins. For ancestral KaiC$^{\alpha}$, KaiC$^{\beta}$, KaiC$^{\varepsilon}$, and KaiC$^{\eta}$, the synthesized genes were cloned into the pET-3a vector (Novagen) with NdeI and BamHI cleaving sites using nucleotides encoding hexagonal histidine (His) at the 3′ end. For extant KaiCs from *Flavobacterium johnsoniae* UW101 and *Rhodopseudomonas palustris* TIE-1 strains, genes were cloned into the pASK-IBA5plus vector (IBA GmbH) with the BsaI cleaving site to overexpress Strep-tagged KaiCs because of the poor yields associated with the GST-tagged form.

Expression and purification of extant and ancestral Kai-proteins

Extant and ancestral KaiCs were expressed in *E. coli* BL21 cells and then purified using affinity chromatography, ion exchange chromatography, and size exclusion chromatography[47] according to the type of fusion tags used. Irrespective of the extant or ancestral types, KaiA and KaiB were purified following the methods used for KaiA^{Se} and KaiB^{Se}, respectively[54].

In vitro rhythm assay

For the in vitro rhythm assay of the extant species, KaiA, KaiB, and KaiC were mixed in Tris-buffer (20 mM Tris, 150 mM NaCl, 5 mM $MgCl_2$, 1 mM DTT, and 0.5 mM EDTA, pH 8.0) containing 1 mM ATP, and the time-evolution of the phosphorylation of KaiC was monitored. The potential oscillation of the respective KaiCs was assessed in the presence of various concentrations of KaiA (0.01, 0.02, 0.04, and 0.08 mg/mL) and a fixed concentration of KaiB (0.04 mg/mL) according to previous observations that the amount of KaiA in the system markedly affects the amplitude or stability of the rhythm[31,48,55]. KaiCs that showed any slight sign of oscillation under either condition exhibited a stable rhythm in the presence of moderate concentrations of KaiA (0.02–0.04 mg/mL) (Supplementary Fig. 3). For the assay of KaiC^{Syn3} from *Synechocystis* sp. PCC 6803 (ID: 093 in Fig. 1a), a chimeric KaiA homolog (protein ID: WP_010873803.1, ~22% identity to KaiA^{Se}) that is not listed in the present KaiA tree but has recently been identified was used together with KaiB^{Syn3} (ID: 179 in Supplementary Fig. 5d)[36]. Similarly, for the assay of KaiC^{Cya2} from *Cyanothece* sp. ATCC 51142 (ID: 085 in Fig. 1a), a KaiA homolog (protein ID: WP_009543244.1, ~17% identity to KaiA^{Se}) and KaiB^{Cya2} (ID: 086 in Supplementary Fig. 5d) were used[36].

For the in vitro rhythm assay of the ancestral forms, KaiA, KaiB, and KaiC were mixed in Tris-buffer (20 mM Tris, 150 mM NaCl, 5 mM $MgCl_2$, 1 mM DTT, and 0.5 mM EDTA, pH 7.0) containing 1 mM ATP at final Kai-protein concentrations listed in Table 1.

ATPase measurements

ATPase measurements were performed by monitoring the accumulation of ADP[47] using an ultrahigh-performance liquid chromatography (UHPLC) system (Chromaster, Hitachi). Ancestral KaiCs and KaiC^{Se} were incubated in a Tris-buffer containing 1 mM ATP at pH 7.0 and pH 8.0, respectively. The ATPase activity of KaiC was defined as the number of hydrolyzed ATP molecules into ADP molecules per KaiC monomer per unit time.

Pre-steady-state ATPase assay

For the pre-steady-state ATPase assay[29], an apo-KaiC monomer was first prepared using a phospho-buffer (50 mM NaH_2PO_4, 150 mM NaCl, 50 mM L-arginine, 50 mM L-glutamic acid, 5 mM $MgCl_2$, and 1 mM DTT, pH 7.8)[56]. Reassembly of KaiC hexamers was induced by mixing the apo-KaiC monomer with the phospho-buffer containing ATP, and the resultant mixture containing 1 mM ATP was immediately subjected to UHPLC analysis for ATPase measurements.

Entrainment by external temperature cycles

Kai-protein oscillators were exposed to temperature cycles[40] of one half of the period length at 40 °C and the other half at 30 °C using an automated sampling device[57]. For each of the A$^{\gamma}$B$^{\gamma}$C$^{\gamma}$ (pH 7.0) and A^{Se}B^{Se}C^{Se} (pH 8.0) sets, the Kai-protein oscillators were reconstituted at 0, 6, and 12 h intervals and incubated at 30 °C for 36, 30, and 24 h, respectively. The pre-incubated samples were subjected to five temperature cycles of 18 h (9 h at 40 °C and 9 h at 30 °C: 9H9L), 20 h (10 h at 40 °C and 10 h at 30 °C: 10H10L), or 24 h (12 h at 40 °C and 12 h at 30 °C: 12H12L) to evaluate the entrainability.

pH and Q_{10} values

The pH of the buffers listed in the main text and in Supplementary Information was measured at 25 °C during buffer preparation. The p*K*a value of Tris is slightly temperature-dependent[58]. We confirmed that Tris buffers with pH 7.0 when prepared at 25 °C change to pH 6.8 at 30 °C and pH 6.6 at 40 °C, and Tris buffers with pH 8.0 at 25 °C change to pH 7.8 at 30 °C and pH 7.6 at 40 °C, as actual measured values at the corresponding temperatures. Therefore, Q_{10} values calculated from data obtained at 30 °C and 40 °C using the corresponding Tris buffers

Table 1 | Kai-protein concentrations for in vitro rhythm assays

Panel	Mixture	T (°C)[a]	C (mg/mL)[b]			Replicate
			KaiA	KaiB	KaiC	
Fig. 1i	$A^{Y}B^{\alpha/\beta}C^{\alpha}$	30	0.04	0.04	0.2	Three replicates from two independent purifications
		40	0.04	0.04	0.2	Three replicates from two independent purifications
	$A^{Se}B^{Se}C^{\alpha}$	30	0.04	0.04	0.2	Three replicates from two independent purifications
Fig. 1j	$A^{Y}B^{\alpha/\beta}C^{\beta}$	30	0.04	0.04	0.2	Three replicates from two independent purifications
		40	0.04	0.04	0.2	Three replicates from two independent purifications
	$A^{Se}B^{Se}C^{\beta}$	30	0.04	0.04	0.2	Three replicates from two independent purifications
Fig. 1k	$A^{Y}B^{Y}C^{Y}$	30	0.04	0.04	0.2	Three replicates from two independent purifications
		40	0.04	0.04	0.2	Three replicates from a single purification
	$A^{Se}B^{Se}C^{Y}$	30	0.04	0.04	0.2	Three replicates from a single purification
Fig. 1l	$A^{\zeta}B^{Y}C^{\zeta}$	30	0.05	0.02	0.2	Three replicates from a single purification
		40	0.06	0.02	0.2	Three replicates from a single purification
	$A^{Se}B^{Se}C^{\zeta}$	30	0.04	0.04	0.2	Three independent purifications
Fig. 1m	$A^{\delta}B^{\delta}C^{\delta}$	30	0.04	0.04	0.2	Three replicates from two independent purifications
		40	0.04	0.04	0.2	Three replicates from two independent purifications
	$A^{Se}B^{Se}C^{\delta}$	30	0.04	0.04	0.2	Three replicates from a single purification
Fig. 1n	$A^{Y}B^{\varepsilon}C^{\varepsilon}$	30	0.04	0.04	0.2	Three replicates from a single purification
		40	0.04	0.04	0.2	Three replicates from a single purification
	$A^{Se}B^{Se}C^{\varepsilon}$	30	0.04	0.04	0.2	Three replicates from two independent purifications
Fig. 1o	$A^{Y}B^{\eta}C^{\eta}$	30	0.04	0.04	0.2	Three replicates from two independent purifications
		40	0.04	0.04	0.2	Three replicates from two independent purifications
	$A^{Se}B^{Se}C^{\eta}$	30	0.04	0.04	0.2	Three replicates from two independent purifications

[a]Temperature of incubated samples.
[b]Concentration of each Kai protein.

could include additional pH-dependent effects, if any, of approximately −0.2 pH units.

In vivo rhythm assays

Synechococcus elongatus PCC 7942 was used as the background strain for this assay. To conduct the in vivo bioluminescence assay and analysis[16], cyanobacterial cells carrying the *kaiBC*-reporter cassette were cultured at 30 °C for 3 days on BG-11 solid medium under constant light (LL) at 100 μmol m^{-2} s^{-1}. After one or three 17-h light/17-h dark treatments, the cells were cultured at 30 °C under LL (45 μmol m^{-2} s^{-1}) at an LED daylight lamp, and bioluminescence profiles were monitored using a photomultiplier tube detector.

X-ray structure analyses of $KaiC^{\beta}$, $KaiC^{Y}$, and $KaiC^{\delta}$

Crystals of $KaiC^{\beta}$, $KaiC^{Y}$, and $KaiC^{\delta}$ were obtained using the sitting-drop vapor diffusion method with 5 mM AMP-PNP. $KaiC^{\beta}$ (3 mg/mL) was mixed with a solution of 18 mM acetic acid and 65 mM sodium malonate (pH 5.7). The cryo-protectant treatment was performed using 30% (w/v) PEG4K. $KaiC^{Y}$ (3 mg/mL) was crystallized in a solution of 0.94 M sodium formate and 1.2 M sodium malonate (pH 8.5), which are both cryo-protectants. $KaiC^{\delta}$ (3 mg/mL) was added to 0.1 M Tris-HCl (pH 7.0), 1 M KCl, and 1.14 M sodium malonate.

$KaiC^{\beta}$, $KaiC^{Y}$, and $KaiC^{\delta}$ crystals were frozen using liquid nitrogen and placed under the cryo-stream of the SPring-8 BL44XU beamline (Harima, Japan). The crystals were exposed to X-ray irradiation at a wavelength of 0.9 Å, and diffraction images were collected by using an EIGER X 16 M detector (Dectris) and the semi-automatic data reduction software, KAMO[59]. Diffraction intensity data were processed using XDS (version Jun 30, 2023)[60]. The initial models for $KaiC^{\beta}$, $KaiC^{Y}$, and $KaiC^{\delta}$ were obtained using the molecular replacement method with MOLREP (version 11.9.02)[61] and the coordinates of the $KaiC^{Se}$ hexamer (PDB ID: 2GBL) as a template. Refinement was achieved using REFMAC5 (version 5.8.0415)[62]. The model was constructed by using COOT (version 0.9.8.7)[63]. PyMOL (Schrödinger) (version 2.5.2) was used for the graphic presentation of the refined models.

The $KaiC^{\beta}$, $KaiC^{Y}$, and $KaiC^{\delta}$ crystals had lattices of $P2_1$ (a = 93 Å, b = 386 Å, c = 108 Å, β = 113°; two hexamers in an asymmetric unit), $P1$ (a = 91 Å, b = 110 Å, c = 167 Å, α = 78°, β = 87°, γ = 82°; single hexamer in an asymmetric unit), and $P2_1$ (a = 92 Å, b = 175 Å, c = 95 Å, β = 97°; single hexamer in an asymmetric unit), respectively.

Reporting summary

Further information on research design is available in the Nature Portfolio Reporting Summary linked to this article.

Data availability

All data needed to evaluate the conclusions in the paper are provided in the paper, the Supplementary Information, and Source Data file. Source data for all the plots, 16S rRNA sequences, and extant Kai-protein sequences are provided with this paper. The atomic coordinates and structure factors have been deposited in the Protein Data Bank with accession codes 8ZN5 ($KaiC^{\beta}$), 8ZN6 ($KaiC^{Y}$), and 8ZN7 ($KaiC^{\delta}$). Accession codes of analyzed published sequence data are available in the Source data file. Source data are provided with this paper.

References

1. Schirrmeister, B. E., Gugger, M. & Donoghue, P. C. Cyanobacteria and the great oxidation event: evidence from genes and fossils. *Palaeontology* **58**, 769–785 (2015).
2. Oliver, T. et al. The evolution and evolvability of photosystem II. *Annu. Rev. Plant Biol.* **74**, 225–257 (2023).
3. Garcia-Pichel, F. et al. Timing the evolutionary advent of cyanobacteria and the later great oxidation event using gene phylogenies of a sunscreen. *Mbio* **10**, e00561-19 (2019).

4. Nishihara, A., Tsukatani, Y., Azai, C. & Nobu, M. K. Illuminating the coevolution of photosynthesis and bacteria. *Proc. Natl. Acad. Sci. USA* **121**, e2322120121 (2024).
5. Shih, P. M., Hemp, J., Ward, L. M., Matzke, N. J. & Fischer, W. W. Crown group oxyphotobacteria postdate the rise of oxygen. *Geobiology* **15**, 19–29 (2017).
6. Betts, H. C. et al. Integrated genomic and fossil evidence illuminates life's early evolution and eukaryote origin. *Nat. Ecol. Evol.* **2**, 1556–1562 (2018).
7. Bekker, A. et al. Dating the rise of atmospheric oxygen. *Nature* **427**, 117–120 (2004).
8. Kirschvink, J. L. Late proterozoic low-latitude global glaciation: the snowball Earth. in *The Proterozoic Biosphere: A Multidisciplinary Study* (eds Schopf, J. W., Klein, C. & Maris, D.) (Cambridge University Press, 1992).
9. Hoffman, P. F. et al. Snowball Earth climate dynamics and cryogenian geology-geobiology. *Sci. Adv.* **3**, e1600983 (2017).
10. Macdonald, F. A. et al. Calibrating the cryogenian. *Science* **327**, 1241–1243 (2010).
11. Scott, C. et al. Tracing the stepwise oxygenation of the Proterozoic ocean. *Nature* **452**, 456–459 (2008).
12. Och, L. M. & Shields-Zhou, G. A. The neoproterozoic oxygenation event: environmental perturbations and biogeochemical cycling. *Earth Sci. Rev.* **110**, 26–57 (2012).
13. Edgar, R. S. et al. Peroxiredoxins are conserved markers of circadian rhythms. *Nature* **485**, 459–464 (2012).
14. Wu, H. B., Murray, N., Menou, K., Lee, C. & Leconte, J. Why the day is 24 hours long: the history of Earth's atmospheric thermal tide, composition, and mean temperature. *Sci. Adv.* **9**, eadd2499 (2023).
15. Dunlap, J. C. Molecular bases for circadian clocks. *Cell* **96**, 271–290 (1999).
16. Ishiura, M. et al. Expression of a gene cluster as a circadian feedback process in cyanobacteria. *Science* **281**, 1519–1523 (1998).
17. McClung, C. R., Fox, B. A. & Dunlap, J. C. The Neurospora clock gene frequency shares a sequence element with the Drosophila clock gene period. *Nature* **339**, 558–562 (1989).
18. Strayer, C. et al. Cloning of the Arabidopsis clock gene TOC1, an autoregulatory response regulator homolog. *Science* **289**, 768–771 (2000).
19. Gekakis, N. et al. Role of the CLOCK protein in the mammalian circadian mechanism. *Science* **280**, 1564–1569 (1998).
20. Akiyama, S. Structural and dynamic aspects of protein clocks: how can they be so slow and stable? *Cell Mol. Life Sci.* **69**, 2147–2160 (2012).
21. Swan, J. A., Golden, S. S., LiWang, A. & Partch, C. L. Structure, function, and mechanism of the core circadian clock in cyanobacteria. *J. Biol. Chem.* **293**, 5026–5034 (2018).
22. Nakajima, M. et al. Reconstitution of circadian oscillation of cyanobacterial KaiC phosphorylation in vitro. *Science* **308**, 414–415 (2005).
23. Nishiwaki, T. et al. A sequential program of dual phosphorylation of KaiC as a basis for circadian rhythm in cyanobacteria. *EMBO J.* **26**, 4029–4037 (2007).
24. Rust, M. J., Markson, J. S., Lane, W. S., Fisher, D. S. & O'Shea, E. K. Ordered phosphorylation governs oscillation of a three-protein circadian clock. *Science* **318**, 809–812 (2007).
25. Akiyama, S., Nohara, A., Ito, K. & Maéda, Y. Assembly and disassembly dynamics of the cyanobacterial periodosome. *Mol. Cell* **29**, 703–716 (2008).
26. Kageyama, H. et al. Cyanobacterial circadian pacemaker: Kai protein complex dynamics in the KaiC phosphorylation cycle in vitro. *Mol. Cell* **23**, 161–171 (2006).
27. Tseng, R. et al. Structural basis of the day-night transition in a bacterial circadian clock. *Science* **355**, 1174–1180 (2017).
28. Chavan, A. G. et al. Reconstitution of an intact clock reveals mechanisms of circadian timekeeping. *Science* **374**, eabd4453 (2021).
29. Abe, J. et al. Atomic-scale origins of slowness in the cyanobacterial circadian clock. *Science* **349**, 312–316 (2015).
30. Terauchi, K. et al. ATPase activity of KaiC determines the basic timing for circadian clock of cyanobacteria. *Proc. Natl. Acad. Sci. USA* **104**, 16377–16381 (2007).
31. Furuike, Y. et al. Cross-scale analysis of temperature compensation in the cyanobacterial circadian clock system. *Commun. Phys.* **5**, 75 (2022).
32. Dvornyk, V., Vinogradova, O. & Nevo, E. Origin and evolution of circadian clock genes in prokaryotes. *Proc. Natl. Acad. Sci. USA* **100**, 2495–2500 (2003).
33. Schmelling, N. M. et al. Minimal tool set for a prokaryotic circadian clock. *BMC Evol. Biol.* **17**, 169 (2017).
34. Pitsawong, W. et al. From primordial clocks to circadian oscillators. *Nature* **616**, 183–189 (2023).
35. Ma, P., Mori, T., Zhao, C., Thiel, T. & Johnson, C. H. Evolution of KaiC-dependent timekeepers: a proto-circadian timing mechanism confers adaptive fitness in the purple bacterium rhodopseudomonas palustris. *PLoS Genet.* **12**, e1005922 (2016).
36. Köbler, C. et al. Two KaiABC systems control circadian oscillations in one cyanobacterium. *Nat. Commun.* **15**, 7674 (2024).
37. Dvornyk, V. & Mei, Q. M. Evolution of kaiA, a key circadian gene of cyanobacteria. *Sci. Rep.* **11**, 9995 (2021).
38. Halevy, I. & Bachan, A. The geologic history of seawater pH. *Science* **355**, 1069–1071 (2017).
39. Belkin, S., Mehlhorn, R. J. & Packer, L. Proton gradients in intact cyanobacteria. *Plant Physiol.* **84**, 25–30 (1987).
40. Yoshida, T., Murayama, Y., Ito, H., Kageyama, H. & Kondo, T. Nonparametric entrainment of the in vitro circadian phosphorylation rhythm of cyanobacterial KaiC by temperature cycle. *Proc. Natl. Acad. Sci. USA* **106**, 1648–1653 (2009).
41. Furuike, Y. et al. Elucidation of master allostery essential for circadian clock oscillation in cyanobacteria. *Sci. Adv.* **8**, eabm8990 (2022).
42. Kim, Y. I., Dong, G., Carruthers, C. W. Jr., Golden, S. S. & LiWang, A. The day/night switch in KaiC, a central oscillator component of the circadian clock of cyanobacteria. *Proc. Natl. Acad. Sci. USA* **105**, 12825–12830 (2008).
43. Pattanayek, R. et al. Visualizing a circadian clock protein: crystal structure of KaiC and functional insights. *Mol. Cell* **15**, 375–388 (2004).
44. Young, M. W. & Kay, S. A. Time zones: a comparative genetics of circadian clocks. *Nat. Rev. Genet.* **2**, 702–715 (2001).
45. Kushige, H. et al. Genome-wide and heterocyst-specific circadian gene expression in the filamentous Cyanobacterium *Anabaena* sp. strain PCC 7120. *J. Bacteriol.* **195**, 1276–1284 (2013).
46. Arbel-Goren, R. et al. Robust, coherent, and synchronized circadian clock-controlled oscillations along Anabaena filaments. *Elife* **10**, e64348 (2021).
47. Mukaiyama, A., Ouyang, D. Y., Furuike, Y. & Akiyama, S. KaiC from a cyanobacterium sp. PCC 7428 retains functional and structural properties required as the core of circadian clock system. *Int. J. Biol. Macromol.* **131**, 67–73 (2019).
48. Ito-Miwa, K., Furuike, Y., Akiyama, S. & Kondo, T. Tuning the circadian period of cyanobacteria up to 6.6 days by the single amino acid substitutions in KaiC. *Proc. Natl. Acad. Sci. USA* **117**, 20926–20931 (2020).
49. Kopp, R. E., Kirschvink, J. L., Hilburn, I. A. & Nash, C. Z. The Paleoproterozoic snowball Earth: a climate disaster triggered by the evolution of oxygenic photosynthesis. *Proc. Natl. Acad. Sci. USA* **102**, 11131–11136 (2005).

50. Woelfle, M. A., Ouyang, Y., Phanvijhitsiri, K. & Johnson, C. H. The adaptive value of circadian clocks: an experimental assessment in cyanobacteria. *Curr. Biol.* **14**, 1481–1486 (2004).
51. Kumar, S., Stecher, G., Li, M., Knyaz, C. & Tamura, K. MEGA X: molecular evolutionary genetics analysis across computing platforms. *Mol. Biol. Evol.* **35**, 1547–1549 (2018).
52. Kanehisa, M. & Goto, S. KEGG: kyoto encyclopedia of genes and genomes. *Nucleic Acids Res.* **28**, 27–30 (2000).
53. Kumar, S. et al. TimeTree 5: an expanded resource for species divergence times. *Mol. Biol. Evol.* **39**, msac174 (2022).
54. Nishiwaki, T. et al. Role of KaiC phosphorylation in the circadian clock system of PCC 7942. *Proc. Natl. Acad. Sci. USA* **101**, 13927–13932 (2004).
55. Nakajima, M., Ito, H. & Kondo, T. In vitro regulation of circadian phosphorylation rhythm of cyanobacterial clock protein KaiC by KaiA and KaiB. *FEBS Lett.* **584**, 898–902 (2010).
56. Mukaiyama, A., Osako, M., Hikima, T., Kondo, T. & Akiyama, S. A protocol for preparing nucleotide-free KaiC monomer. *Biophysics* **11**, 79–84 (2015).
57. Furuike, Y., Abe, J., Mukaiyama, A. & Akiyama, S. Accelerating in vitro studies on circadian clock systems using an automated sampling device. *Biophys. Physicobiol.* **13**, 235–241 (2016).
58. Good, N. E. et al. Hydrogen ion buffers for biological research. *Biochemistry* **5**, 467–477 (1966).
59. Yamashita, K., Hirata, K. & Yamamoto, M. KAMO: towards automated data processing for microcrystals. *Acta Crystallogr. D Struct. Biol.* **74**, 441–449 (2018).
60. Kabsch, W. XDS. *Acta Crystallogr. D Biol. Crystallogr.* **66**, 125–132 (2010).
61. Vagin, A. & Teplyakov, A. MOLREP: an automated program for molecular replacement. *J. Appl. Crystallogr.* **30**, 1022–1025 (1997).
62. Murshudov, G. N. et al. REFMAC5 for the refinement of macromolecular crystal structures. *Acta Crystallogr. D Biol. Crystallogr.* **67**, 355–367 (2011).
63. Emsley, P., Lohkamp, B., Scott, W. G. & Cowtan, K. Features and development of Coot. *Acta Crystallogr. D Biol. Crystallogr.* **66**, 486–501 (2010).
64. Buick, R., Des Marais, D. J. & Knoll, A. H. Stable isotopic compositions of carbonates from the Mesoproterozoic Bangemall Group, northwestern Australia. *Chem. Geol.* **123**, 153–171 (1995).

Acknowledgements

Diffraction data were collected at beamline BL44XU at the SPring-8 facility under the proposals 2021A6700, 2021B6602, 2023A6500, 2023B6842, and 2024A6930. This research was partly supported by the Platform Project for Supporting Drug Discovery and Life Science Research (BINDS) from AMED under grant number JP21am0101072 (support number 0583). This study was supported by Grants-in-Aid for Scientific Research (22H04984 to S.A., A.M., and Y.F., 17H06165 to S.A. and Y.F., 24H02301 to S.A., 22K15051 to Y.F., 19K16061 to Y.F., and 22K06175 to A.M.), Takeda Science Foundation (to S.A.), and Toyoaki Scholarship Foundation (to S.A.).

Author contributions

A.M., Y.F., and S.A. conceived the project. S.A., A.M., and Y.F. supervised the project. A.M. and Y.F. performed most of the biochemical experiments and analysis. A.M., Y.F., Y.O., and K.H. performed rhythm and ATPase assays. Y.O. performed the nucleotide-exchange experiments. K.K. and K.H. performed temperature-entrainment experiments. Y.F. collected the diffraction data and analyzed it with input from E.Y. K.I.-M. performed in vivo experiments. S.A., A.M., and Y.F. drafted the manuscript. All the authors read and commented on the manuscript.

Competing interests

The authors declare no competing interests.

Additional information

Supplementary information The online version contains supplementary material available at https://doi.org/10.1038/s41467-025-59908-7.

Correspondence and requests for materials should be addressed to Atsushi Mukaiyama, Yoshihiko Furuike or Shuji Akiyama.

Peer review information *Nature Communications* thanks the anonymous reviewers for their contribution to the peer review of this work. A peer review file is available.